/ />   ( )

Extended-Testing of Xenon Ion Thruster Hollow Cathodes

Timothy R. Sarver-Verhey
Sverdrup Technology, Inc.
Lewis Research Center Group
Brook Park, Ohio

July 1992

NASA

Extended Testing of Xenon Ion Thruster Hollow Cathodes

Timothy R. Sarver-Verhey
Sverdrup Technology Group
NASA Lewis Research Center
Brook Park, OH 44142

A hollow cathode wear-test of 508 hours was successfully completed at an emission current of 23.0 A and a xenon flow rate of 10 Pa-L/s. This test was the continuation of a hollow cathode contamination investigation. Discharge voltage was stable at 16.7 V. The cathode temperature averaged 1050 oC with a 7% drop during the wear-test. Discharge ignition voltage was found to be approximately 20 V and was repeatable over four starts. Post-test analyses of the hollow cathode found a much improved internal cathode condition with respect to earlier wear-test cathodes. Negligible tungsten movement occurred and no formation of mono-barium tungstate was observed. These results correlated with an order-of-magnitude reduction in propellant feed-system leakage rate. Ba2CaWO6 and extensive calcium crystal formation occurred on the upstream end of the insert. Ba-Ca compound depositions were found on the Mo insert collar, on the Re electrical leads, and in the gap between the insert and cathode wall. This wear-test cathode was found to be in the best internal condition and had the most stable operating performance of any hollow cathode tested during this contamination investigation.

NOMENCLATURE

A	= emitting surface area, m^2
I_e	= emission current, A
I_{htr}	= heater current, A
P_{cond}	= conduction power losses, W
P_{htr}	= heater power, W
P_{in}	= input power, W
P_{out}	= output power, W
P_{rad}	= radiation power losses, W
t	= time, hours
T_{cath}	= cathode tube temperature, ^oC
V_d	= discharge voltage, V
V_{htr}	= heater voltage, V
ϵ	= total surface emissivity
σ	= Stefan-Boltzman coefficient, $5.67 \times 10^{-8}\ W/K^4\text{-}m^2$

Subscripts

i	= initial state
f	= final state

INTRODUCTION

Hollow cathodes, operating on inert gases and emitting several to several tens of amperes of current, have experienced destructive effects during extended testing. The causes of hollow cathode deterioration are believed to be oxygen contamination of the propellant feed-system by air leakage and surface outgassing and excessive cathode operating temperatures.

Oxidation of components and deposition of material in the cathode orifices and on the internal surfaces have resulted in degraded performance and cathode failure, as has been reported by several researchers.[1-6] Extended testing of hollow cathodes operating on inert gases at several amperes of emission current for longer than 1,000 hours has been limited to two xenon ion thruster life-tests. Beattie et al. reported on a 4,350 hr. test of a xenon ion propulsion subsystem operated at 1.4 kW. The main discharge hollow cathode was operated at an emission current of 6.3 A and experienced cathode orifice erosion.[7] Brophy and Garner reported on the successful completion of a 5,000 hour test of a hollow cathode operated on xenon in an ion thruster simulator at an emission current of 25 A.[8] Operating parameters such as discharge voltage and ignition voltage varied considerably during the test and cathode insert brightness temperature was found to be approximately 1500 ^oC throughout the test. Substantial material deposition was found on the cathode insert surface in post-test examination. Consequently, concerns have arisen about the ability of hollow cathodes to provide stable operation with long life.

An effort was therefore begun to alleviate cathode degradation due to oxygen contamination by developing criteria and procedures to ensure that cathode life-limitations were minimized. This effort consisted of a program of extended cathode testing in configurations designed to simulate 30

cm ion thruster discharge chambers. Under this program, wear-test experience with two hollow cathodes, operated on xenon propellant for approximately 500 hours each, has been reported.[4] Operational characteristics of the hollow cathodes were measured during the wear-tests and post-test microanalyses of the cathode interior surfaces documented component degradation resulting from discharge operation. Several destructive phenomena, particularly tungsten removal and deposition, were found on these wear-test hollow cathodes, referred to hereafter as WT-I and WT-II. It was found that by improving the vacuum integrity of the propellant feed-system and implementing alternate cathode activation procedures for wear-test WT-II, the internal condition of the hollow cathode and its operation were improved. Criteria were developed from these results to provide guidelines to ensure safe hollow cathode operation.

This paper reports on the first extended test of a hollow cathode in a newly established cryogenically pumped vacuum facility at NASA Lewis Research Center (LeRC). The test configuration of this hollow cathode, referred to as WT-III, further implemented criteria developed from the earlier work. Along with improvements in the propellant feed-system, new procedures were also implemented. The extended test reported here lasted for 508 hours. The hollow cathode was operated at 23.0 A and 10 Pa-L/s (6.1 sccm (STP), 0.55 mg/s) of xenon flow to enable comparison of operation and final condition with earlier tests. The propellant feed-system leakage rate was used as the figure of merit for quantitative measure of contamination experienced by the cathode. Post-test microanalyses were performed to document the final internal state of the cathode.

APPARATUS

Hollow Cathode Design specifications of the hollow cathode are summarized in Table I. The cathode, shown schematically in Fig. 1, consisted of a 0.64 cm dia. Mo/Re tube, 10.2 cm long, with a thoriated tungsten orifice plate electron-beam welded to one end. A 0.15 cm dia. orifice with a 45° half-angle chamfer on the downstream surface was electron-discharge machined into this plate. The insert, a sintered tungsten cylinder impregnated with $4BaO \cdot CaO \cdot Al_2O_3$, was inserted into the tube. Rhenium electrical leads, attached to the rear of the insert, were spot-welded to the interior of the upstream end of the body tube. These leads provided the electrical contact and maintained the position of the insert at the downstream end of the body tube.

A helical-wound sheathed tantalum heater used for cathode activation and ignition was friction-fitted on the outside of the body tube, over the region occupied by the insert.[3] Eleven layers of 0.013 cm thick Ta foil were tightly wrapped around the heater to enhance heater operation by reducing radiated power losses. A type R (Pt-Pt/Rh) thermocouple was spot-welded to the external surface of the cathode body tube, immediately upstream of the orifice plate weld. Tantalum foil was spot-welded over the thermocouple junction to preclude plasma interactions.

A gas-tight connection to the cathode was made with a flexible graphite compression fitting. This fitting was mounted on a thermally-isolating flange which formed the downstream end of the cathode plenum. This plenum enabled determination of internal cathode pressure as the plenum pressure was calculated to be within 4% of the cathode pressure. The cathode plenum consisted of a 3.3 cm I.D. stainless steel tube with a length of 8.3 cm. At the wear-test operating point, the cathode plenum pressure was approximately 690.0 Pa (5.2 Torr). The plenum was mounted to the vacuum test flange with a pressure transducer mounted on the atmospheric side.

Discharge chamber simulator In order to approximate the geometric and electromagnetic conditions of the 30 cm ring-cusp ion thruster, the cathode was mounted inside a discharge chamber simulator, shown schematically in Fig. 2. The simulator was fabricated from 0.16 cm thick carbon steel. The front plate of the chamber (opposite the cathode) was electrically isolated from the rest of the discharge chamber to simulate the thruster screen grid which is typically at cathode potential. This front plate had a large center aperture over which was mounted a restrictor plate with a 2.5 cm orifice. This restrictor was used to increase the internal discharge chamber pressure to approximate that in an operating ion thruster. With a xenon cathode flow rate of 10.0 Pa-L/s, the chamber

pressure was maintained between 0.34 and 0.44 Pa. The remaining surfaces of the chamber were connected to the positive side of the discharge supply. Three rings of rare-earth (Sm_2Co_{17}) magnets identical to those used in 30 cm ion thruster testing[3] were mounted on the anode potential portion of the chamber wall to provide an equivalent magnet field as in a ring-cusp ion thruster (see Fig. 2). The magnet rings had alternating polarity to insure that a confining magnetic field was formed inside the discharge chamber. The hollow cathode mounted in the plenum was admitted into the discharge chamber through a hole in the backplate. The plane of the cathode orifice was located approximately 8.0 cm downstream of the backplate.

Propellant Feed-system The propellant gas feed-system is shown schematically in Fig. 3. The feed-lines were fabricated from 0.64 cm diameter stainless-steel tubing which had an electro-polished surface finish of 38 μm RMS. The overall length and volume of the feed-line from xenon bottle to cathode plenum was 2.54 m and 1.0×10^{-4} m^3 respectively. All fittings used ultra-high vacuum metal gasket seals, except where transducer installation required O-ring fittings. A lithium-based organometallic polymer gas purifier was installed upstream of the flow monitoring and control devices. This purifier was specified by the vendor to obtain a purity of <10 ppb for oxygen and water vapor, with a maximum effluent contamination of 15 ppm. The internal pressure of the feed-line was greater than ambient pressure in the feed-line segment upstream of the flow control valve and below ambient pressure in the remainder. Two pressure transducers, a Pirani thermocouple gauge and an Capacitance manometer, were mounted in the feed-line to monitor pressures during leakage rate tests and cathode operation. Bypass lines were included between the cathode plenum and the flow control valve and upstream of the flow control valve in order to speed evacuation of the feed-system when pumping down from atmosphere.

Propellant Research grade xenon (99.995%) gas was used throughout the wear-test and the pre- and post-test parametric testing. The xenon delivery pressure was maintained at 170 kPa (10 psig).

Power Supplies Two power supplies were used to operate the hollow cathode. A 25 V, 15 A current-regulated supply provided the required 120 W for the cathode heater during activation and starting. A 60 V, 120 A current-regulated power supply provided both the necessary voltage for ignition and maintenance of the discharge. The cathode, discharge chamber front-plate, and all test-port surfaces were maintained at facility ground while the discharge chamber was connected to the positive output of the discharge supply and electrically isolated from the test port. The electrical connections are indicated in the schematic in Fig. 2.

Instrumentation The parameters monitored over the course of the test were the discharge voltage and current, as well as the noise on each, xenon mass flow rate, the cathode temperature, the facility, anode, and cathode plenum pressures. The cathode temperature measurements were made with the type R thermocouple mounted on the cathode body tube. Bayard-Alpert ion gauges were used to monitor the facility and discharge chamber pressures. The discharge chamber ion gauge was able to sense the chamber pressure via a 2.5 cm dia. pyrex tube running through the chamber backplate and the ion gauge feedthrough. A capacitance manometer was used to measure cathode plenum pressure. All parameters listed above, except for discharge noise, were recorded at 15 minute intervals during the wear-test with a data-logger.

Vacuum Facility The discharge chamber simulator was mounted in a test port attached to a 30.5 cm dia. six-way vacuum cross evacuated with a helium refrigerator cryo-pump. The test port and bell jar are shown with the discharge chamber simulator installed in the photograph in Fig. 4. The vacuum pump had a xenon pumping capacity of approximately 1100 L/s and was capable of collecting up to 2000 L of xenon. This total capacity allows up to 5500 hours of continuous testing at the wear-test xenon mass flow rate before regeneration of the cryogenic surface is required. The facility had a base-pressure of approximately 1.3×10^{-5} Pa and a operating pressure of 1.5×10^{-2} Pa at the test conditions described below.

TEST PROCEDURES

3

Pre-test procedures   Prior to the installation of the cathode, a bake-out of the propellant feed-system was performed to facilitate outgassing of water vapor trapped on the interior tubing surfaces. Heat tape was wrapped over the feed-line and powered to raise the tube temperature to 75 $^{\circ}$C. All bypass lines were open to the bell jar vacuum to remove water outgassed from the feed-line surfaces. The bake-out lasted approximately 17 hours. During installation of the test cathode, the propellant feed-system was isolated to prevent recontamination of the feed-lines. The mass flow transducer was calibrated before and after the test with a bubble flow calibrator using xenon. Insert activation was initiated once the cathode was at a vacuum level of approximately 2×10^{-4} Pa and feed-line pressure was below 10^{-2} Pa. The procedure used at NASA-LeRC, shown graphically in Fig. 5, was derived from an activation procedure developed during the Solar Electric Propulsion Subsystem (SEPS) program.[9] Figure 5 shows the activation procedure and the cathode pre-heat for ignition. After activation, a 0.5 hour 1050 $^{\circ}$C pre-heat of the cathode was performed prior to discharge ignition to insure repeatable, low-voltage ignition.

Cathode operating characteristics were documented once the cathode discharge was ignited. The current-voltage characteristics and the cathode temperature behavior were measured. In addition, the dynamic characteristics of the discharge power supply were characterized prior to the wear-test and monitored throughout the test. These dynamic measurements were made with a digital storage oscilloscope with voltage and inductive current probes attached to the discharge power supply feedthrough at the test flange.

Propellant Feed-System Character-ization   In order to characterize the contamination level within the propellant feed-system due to air leakage through the fittings and outgassing from the internal surfaces, pressure-rise testing was performed. Pressure-rise tests consisted of evacuating the feed-system to below 10^{-2} Pa, then isolating the feed-line from the bell jar vacuum and monitoring the rise in pressure over time with the two pressure transducers discussed above. This pressure rise was taken to be due to leakage in through the fittings and outgassing from the internal surfaces. However, outgassing was not detectable over multiple tests performed prior to the wear-test, indicating that the outgassing contribution to the total contamination was insufficient to distinguish from the contribution due to physical leakage. This behavior differed from earlier wear-tests where the outgassing contribution was apparent during the pressure-rise tests.[4]

The physical leakage was quantified by measuring the pressure rise with time using the change starting at t > 22 hours and continuing for approximately 40 hours. The pressure change during the first 28 hours was neglected as a precaution against any outgassing contribution. An effective leakage rate of 4.7×10^{-6} Pa-L/s was determined for the pre-test feed-system. Post-test measurements found an improved leakage rate of 3.3×10^{-6} Pa-L/s which may have been the result of continually removal of contaminants during the wear-test.

Post-test Microanalysis Techniques   Post-test analyses of the cathode were performed with four different techniques. First, a boroscope was used to visually examine the internal condition of the hollow cathode. Straight-on and right-angle microbore probes enabled visual inspection of nearly all on the internal cathode surfaces. Second, scanning electron microscopy (SEM) was used for physical examination of cathode and insert surfaces by secondary electron emission (SE) and back-scattered electron emission (BSE) spectroscopy. Third, energy dispersive x-ray analysis (EDS) was used to determine the elemental composition of the surfaces. Finally, x-ray diffraction analysis (XRD) was used for composition determination of materials found on the internal surfaces. It should be noted that the SEM, EDS, and XRD techniques measure material that exists at depths of 1 to 100 μm of the surface. Surfaces as discussed in this report will refer to this region. Surface formations of mono-layer thicknesses are undetectable with the techniques utilized.

OPERATIONAL RESULTS

Propellant Feed-System Condition   The average leakage rate of 4.0×10^{-6} Pa-L/s indicated a 170-fold and a 30-fold improvement in system cleanliness over the two previous wear-test feed-systems.[4] The average leakage

4

rate of the feed-system and other characteristics of this configuration are compared to those from two previous wear-tests, WT-I and WT-II, in Table II. This leakage rate indicated approximately 0.4 ppm of air contamination at the test mass flow rate of 10 Pa-L/s. Neglecting nitrogen as a contaminant, then the total O_2 and H_2O contamination was approximately 0.1 ppm. This contamination level was lower than the 1 ppm O_2 and 2 ppm H_2O indicated by vendor analysis of the xenon. In the two earlier wear-tests, the contamination contribution from the leakage rates were always substantially higher than that of the propellant; 61 ppm for test WT-I and 10 ppm for test WT-II. In those tests, the xenon contribution to total contamination was neglected. For this wear-test, WT-III, xenon gas was the primary source of contamination. The total contaminant which could reach the cathode due to contributions from the xenon and the feed-system was on the order of 1 ppm. The gas purifier was installed to remove gas contamination as well as contributions from the segment of the feed-system upstream of the purifier. Although vendor specifications stated that contamination levels would be reduced to less than 10 ppb, the quantitative effectiveness of the purifier on reduction of contaminants remains to be determined.

Wear-Test History Prior to beginning the wear-test, the cathode was operated for 6 hours, during which performance data were obtained at a fixed mass flow rate. The cathode experienced two shut-downs during the test, the first at hour 275 and the second at hour 353. The first shutdown occurred due to irregular behavior of the discharge power supply which resulted in the discharge current climbing from 23.0 A to 30 A over a 2.5 hour period. Limits on the supply output then triggered a safety relay and shut off the discharge. The cathode was restarted without any problems and the discharge supply performed normally for the remainder of the test. The cause of this shutdown was found to be due to a poor connection in the current-regulation circuit. The second shutdown was not preceded by a current rise or any other parameter change which lasted sufficiently long enough to be recorded by the data-logger. The discharge was off, but open-circuit voltage of the supply was still on after shutdown. The cause of the second shutdown is unknown at this time. The cathode restarted normally after the shutdown and the

test was resumed. With 508 hours of operation at 23.0 A, the cathode wear-test was voluntarily terminated. After the wear-test, performance characterization was performed over a 4 hour period. In addition, the cathode was restarted after 48 hours in order to document starting characteristics and was operated for approximately 0.5 hours. The hollow cathode was then removed from the test facility for examination.

Discharge Characteristics The hollow cathode was tested parametrically before and after the extended-test at a fixed xenon flow rate of 10 Pa-L/s. The measured I_e-V_d and I_e-T_{cath} characteristics are shown in Fig. 6. For the I_e-V_d characteristic, the post-test discharge voltages experienced a 3.0% average rise over the pre-test values over the range of emission currents. Equilibration of the chemical processes at the insert surface was suspected to be the cause of the increase in discharge voltage since the change appeared to have occurred during the beginning of the wear-test. By hour 72 of the test, the discharge voltage had increased from 16.4 V to a stable value of 16.7 V where it remained. Figure 7 shows a plot of the discharge voltage and emission current over the course of the wear-test. The discharge voltage varied by approximately 1.0% during the test. Note that variations in emission current were not reflected in the voltage behavior. The two spikes at hour 275 and 353, respectively indicated the two power supply shutdowns experienced during the wear-test. During both shut-downs, the discharge voltage rose to the open-circuit voltage of approximately 40 V. Figure 7 also indicates the emission current rise prior to the first shutdown. The discharge voltage recovered to the nominal value upon restarting the hollow cathode after both of the shutdowns. The power supply noise level (peak-to-peak) was measured to be 3.0% for emission current and 6.0% for discharge voltage. These noise levels remained constant throughout the wear-test.

The cathode tube temperature decreased from a high of 1090 °C to a low of 1025 °C, as seen in Fig. 8. This decrease was approximately 7.0% over the course of the wear-test. Likewise, cathode tube temperatures were an average of 8.0 % lower after the wear-test over the range of tested emission currents of the I_e-T_{cath} characteristic, as indicated in Fig. 6. While data were not available to determine the cause

5

of this change, a possibility was the change in the cathode heater over the course of the test. Evaluation of the pre- and post-test data supports this hypothesis, and it is discussed in detail in the Appendix. Changes in the thermocouple contact resistance were monitored by measuring the resistance between thermocouple leads and cathode assembly before and after the wear-test. No resistance changes were discernable.

Discharge ignition was required 3 times during the wear-test and once after the completion of the test. In all cases, the required voltage for ignition was between 19.0 and 21.6 V, substantially lower than the several hundred volts required in prior cathode tests.[1,3,8,10] The consistent ignition voltage implied that negligible changes to the cathode occurred during the wear-test.

DISCUSSION OF HOLLOW CATHODE BEHAVIOR AND CHANGES

Improved Cathode Operation Cathode WT-III showed several improvements in cathode operation over the results of tests WT-I and WT-II. First, discharge voltage was approximately constant over the test, experiencing only a 1.8% voltage rise during the first 72 hours. This was the first time steady discharge voltage behavior had been observed in these hollow cathode contamination studies. One effect which may have contributed to discharge voltage stability was the type of vacuum pump employed in the bell jar. By using a He refrigerator cryo-pump, it was not possible for the anode and cathode surfaces to be coated with decomposed diffusion pump oil. While cryo-pump use may be important to cathode operation, the impact of an inherently cleaner testing environment remains to be characterized, as well as decoupled from cathode-related performance.

Cathode ignition voltage was consistently low throughout the test and never exceeded 22 V. While this low ignition voltage behavior could be an indicator of improved cathode condition, it also may have been a result of a proper cathode pre-heat. This pre-heat step was employed to insure that the cathode (as inferred from tube temperature measurements) was at the prescribed operating temperature of the impregnated insert[11] during each ignition. Constant monitoring of the cathode temperature enabled adjustment of the cathode heater power as needed due to changes in the heater performance. The pre-test heater power required to raise the cathode tube temperature to 1050 °C within 30 minutes was 108.0 W. After the test, the heater required 117.0 W to reach the same temperature over the same time period. Using the power level from the pre-test point would have resulted in igniting the discharge with the cathode temparture approximately 30 °C below 1050 °C. Previous results by other researchers suggested that with a lower cathode temperature prior to ignition, the ignition voltage requirements are greater and less repeatable.[12] Consequently, stringent adherence to the prescribed pre-heat procedure was believed to contribute to repeatable ignition though the exact behavior of cathode ignition with remains to be quantified. Additionally, using cathode temperatures as guidelines rather than heater power levels may have been similarly benefical during the cathode activation procedure.

The cathode operational improvements continued a trend observed in the last report on this work.[4] Figure 9 shows the discharge voltages of the three wear-tests WT-I, WT-II, and WT-III. As indicated, the WT-III discharge voltage was the most stable of all the tests. The WT-I voltage showed the largest variation which was believed to correspond to the substantial cathode changes. Cathode WT-II's discharge voltage experienced a monotomic decrease from 22.6 V to 18.0 V during the 478 hour test.

The cathode tube temperatures for these tests are shown in Fig. 10. While cathode WT-III's temperature was not the most stable, it was the lowest average temperature of the three at 1050 °C. The temperature of cathode WT-I showed the same erratic behavior as the discharge voltage and had the highest average temperature at 1200 °C. Cathode WT-II's temperature was the most stable, but ran at a high average temperature of 1100 °C.

The improved operation of cathode WT-III was attributed to upgrades to the test configuration in line with the criteria suggested in the previous report[4] as well as the use of a gas purifier. The improvements incorporated into

the WT-III test are listed in Table II along with equivalent information on the WT-I and WT-II tests. Further improvements possible with the WT-III test configuration include improving the feed-system bake-out procedures, positioning the gas purifier as close as possible to the cathode, and use of metal-seal fittings throughout the feed-system.

Hollow Cathode Condition A schematic summary of the observed changes is provided in Fig. 11. This schematic is a qualitative lay-out of the observed phenomena; photos of different regions are indicated by the encircled figure numbers. Also indicated are the elements and compounds determined in their relative positions by EDS and XRD microanalysis techniques, respectively. The observed phenomena on the internal surface of the cathode WT-III, along with the earlier wear-test cathodes, WT-I and WT-II, are summarized in Table III.

Figs. 12 a and 12 b show the cathode before and after the wear-test. As can be seen, the orifice plate was roughened by ion bombardment occurring during the test. However, there were no structural changes in orifice chamfer, channel diameter, or plate weld after 508 hours of discharge operation. Under SEM examination, no deposition or erosion on the orifice chamfer or channel was observed, as indicated in the photograph in Fig. 13.

The only change found on the orifice plate was a ring-like formation of deposited material on the inner surface of the plate, initially observed with the boroscope. Figure 14 is a BSE image photograph of the orifice plate inner surface. The formation varied with radial distance from cathode orifice centerline. Approximately 100 μm from the edge of the orifice channel, a 100 μm wide ring of deposited tungsten metal, approximately 30 μm high, was formed. This metal deposition was structurally identical to previously observed W metal formations found on the cathodes WT-I and WT-II.[4] However, the deposition was substantially less in amount and was limited to the area immediately around the orifice. Further out from the orifice edge, the formation was comprised of particulate deposition composed primarily of tungsten with trace amount of Ba, Ca, Al, and Mo present. The trace levels of Ba and Ca increased with radial distance from the orifice, while the relative particulate size

decreased with increasing distance from the orifice. However, the amounts of these elements were never substantial. This formation stopped at the point on the surface where the insert contacted the orifice plate. A gross correlation between particulate size and Ba and Ca levels can only be speculated at this time. One consequence of the presence of Ba on the orifice inner surface may be to increase the contribution by the orifice plate surface to the total emission current draw from the cathode as a result of a decrease of the orifice plate work function. However, the necessary Ba-O layer for emission enhancement[13] on the orifice plate could not be verified. The test configuration did not allow determination of the relative contributions of different regions of the cathode to the emission current. Therefore, the significance of orifice plate emission relative to total emission current is unknown.

The insert surface was found to be clear of any of the impregnate elements, Ba, Ca, and Al, for approximately 1.9 cm starting from the downstream end. X-ray diffraction analysis found only W on the insert surface in this area. This clear region looked like pristine sintered tungsten as can be seen by comparing the surface of WT-III as shown in Fig. 15 and that of an unactivated type S insert, shown in Fig 16. No structural formations were observed on the insert surface, unlike previous tests where tungsten fibers were observed over varying regions of the insert and cathode surfaces. The only change observed in this region was a small increase in surface porosity. This porosity remains to be quantified, but the the size and density of the pore openings were observed to increase slightly with increasing distance from the downstream end. While a mechanism for this increase in porosity has been proposed[14], insufficient data were available to verify any reaction mechanism and to assess the impact on cathode performance of this surface porosity change.

The reduction in pure tungsten deposition correlated qualitatively with the substantial improvement in system cleanliness. While the quantitative mechanism of tungsten movement is not understood, the continual reduction of oxygen levels within the feed-lines from tests WT-I to WT-III consistently resulted in reduced deposited tungsten. This deposition was of concern because of the possible change in operational behavior of the discharge by

7

interference with the emission process at the insert surface. However, the stable discharge voltage and the consistently low ignition voltage suggested that the emission process did not change during this wear-test, in spite of chemistry occurring on upstream regions of the insert surface where emission was negligible.[15,16]

A Ba-W-Ca compound was found in the cathode tube wall-insert gap approximately one diameter from the orifice plate. Similar gap formations were observed in earlier cathodes and were believed to be the result of impregnate material flowing out of the insert pores during cathode operation.[4] The impregnate remained in this region because of the lack of discharge activity. The material in the gap was very similar in appearance to the impregnate-based material formations on the insert collar.

At the upstream end of the insert, a partially-conductive coating comprised of primarily calcium with trace amounts of Ba, Al, and Mo was found on the surface. The W amount varied with location from trace to comparable to the Ca signal, however the cause for such variation was unknown. Figure 17 shows a BSE photograph of this region. Ca coverage peaked approximately 2.5 mm from the Mo collar at the upstream end of the insert. At this point, the coating showed signs of charging under electron beam bombardment indicating that the coating was an insulator. While amorphous barium-compound layers observed on insert surfaces of cathodes WT-I and WT-II were also insulating, none of the coating observed on WT-III had a similar unifrom layer appearance. At the region of maximum coverage, large crystalline formations composed entirely of calcium were found, as can be seen in Fig. 17. This high level of Ca found throughout the coating and the presences of pure Ca crystals at the insert surface was an entirely new observation. Prior to cathode WT-III, examinations of insert surfaces had turned up little calcium, with barium and tungsten being the primary elements in those layers. Given the relative proportions of components in the impregnate mix, there should have been a substantially larger amount of Ba and an equal amount of Al in this coating region of WT-III. However, these elements were at trace levels. Insufficient data were available to determine the formation mechanism or assess the impact of this Ca coating on cathode operation.

The coating became localized upstream of the formation's primary region, with Ca formations occurring in spots with decreasing density nearer the insert collar. Ba, Al, and Mo levels increased in this region. Di-barium calcium tungstate, Ba_2CaWO_6, was detected via XRD in this region, though the amount of tungstate present was indeterminant. Formation of the mono-barium tungstate, $BaWO_4$, which was observed on all previous wear-tested cathodes,[4] was not detected anywhere on the surface. Formation of both Ba_2CaWO_6 and $BaWO_4$ were expected in the 4:1:1 impregnate chemistry and were among the stable final products when cathode is operated at 1100 °C.[17] However, the lone formation of Ba_2CaWO_6 may indicate a reduction in the calcium content of the impregnate. The relatively large amount of calcium in the impregnate was believed to contribute to a system of chemical reactions which are controlled by $BaWO_4$. The other tungstate, Ba_2CaWO_6, is expected to dominate in chemical reaction system which have lower calcium amounts.[17] Consequently, the large amount of Ca found on the insert surface may indicate calcium loss from the impregnate, thus allowing a Ba_2CaWO_6-dominant reaction system. Regardless of the particular form of the tungstate, excessive formation of the compound has been considered to be a life-limiting factor. Since Ba_2CaWO_6 formation was found only at the upstream insert end, well away from the discharge region,[15] the tungstate presence on cathode WT-III was believed to have negligible impact on cathode life. However, the significance of Ba_2CaWO_6 formation and its location and the absence of $BaWO_4$ cannot be quantified at this time .

The most substantial deposition observed on this cathode was on the insert Mo collar which is shown in Fig.18. It contained Ba, Al, Ca, and W and was, in part, composed of Ba_2CaWO_6. The composition indicated that the impregnate and its chemical reactants were mobile during testing and that internal cathode pressure-flow conditions were sufficiently stagnate for these compounds to move upstream of its release site. The deposition occurred with differing structures. The downstream side of deposition covered the collar uniformly and

8

continuously, though the insert-side edge appeared to be breaking up. The upstream side of the deposition was rougher, had a greater vertical extent and did not cover the surface as completely. Similar deposited formations were observed on the Re electrical leads upstream of the Mo collar. A possible explanation for the formation of depositions in this location was that the Mo collar and other upstream surfaces were sufficiently cool to induce condensation of the mobile impregmate material. The differing forms of the deposition may have been a consequence of a temperature gradient across the collar. Similarly, this formation on the collar may have been a consequence of the cathode mounting configuration. A thermally isolating mounting flange was used to retard heat loss due to conduction to the test flange. In the two previous test configurations, the cathode mounts were all metal and therefore substantially more conductive than for cathode WT-III. Consequently, the earlier configurations would have experienced a larger temperature gradient across the cathode tube length, including the insert, relative to the present configuration. Without a large temperature gradient across the insert, insert temperature was expected to be higher and more evenly distributed. As a result, formation of the barium and calcium coating was expected to occur further upstream than previously observed since surface temperature low enough for condensation would now occur further along on the insert surface. However, further investigation is required to substantiate this speculation .

Surprisingly, these collar depositions were found to be reactive with atmosphere over the course of the post-test examination. The collar deposition appeared to grow in volume and the surface fractured as the free elements, i.e. Ba and Ca, in the compound oxidized over a four week period of exposure to atmopshere. The impact of these post-test reactions on the collar deposition was apparently limited to increasing the oxygen content, since no distinct compounds were identifiable. As a result of this observed reactivity, it is suggested that precautions be implemented to reduce or eliminate these post-test reactions.

CONCLUDING REMARKS

A 508-hour wear-test of a xenon hollow cathode was successfully completed in a new vacuum facility which provided greatly reduced contamination levels. This experiment was the latest test in a hollow cathode contamination investigation. The test configuration was modified to better simulate a main discharge cathode in a 30 cm ion thruster. The propellant feed-system was fabricated from high vacuum components, a gas purifier was installed, and procedures were introduced to reduce oxygen contamination levels which would degrade the hollow cathode performance and lifetime. These improvements resulted in a 30-fold reduction in the measured air leakage rate of the feed-system from the previous wear-test.

During the wear-test, the discharge voltage was relatively stable at 16.7 V with a standard deviation of 0.7%. Cathode tube temperature as measured by a thermocouple averaged 1050 $^{\circ}$C and experienced a 7% drop over the wear-test from a high of 1090 $^{\circ}$C. This average temperature drop was believed to be a result of changes in the heater surface emissivity and not due to changes in the cathode condition. The discharge ignition voltage was consistently low with values between 19.0 and 21.6 V.

The post-test condition of cathode WT-III was substantially improved over that of prior wear-tests. The cathode experienced several internal changes during the test: small, highly localized W metal deposition on the orifice plate, Ba- and Ca-based compound and Ca crystal coating of the upstream insert surface, formation of Ba_2CaWO_6 on the insert surface, and impregnate material-based deposition on the upstream Mo collar, Re electrical lead, and in the cathode wall-insert gap. While the significance of the insert collar deposition, the formation of Ba_2CaWO_6, and the substantial amount of calcium detected on the insert surface are unknown at this time, none of the observed phenomena were found to impact cathode performance for total operating time of 508 hours. The largest change in cathode and system perfomance was believed to have resulted from changes in the surface condition of the heater. Consequently, facility effects impacting heater operation should be addressed in future work to resolve the measured deterioration.

9

APPENDIX

Determination of Emissivity Change in Heater Surface

Observed changes in heater performance and wear-test cathode temperature were evaluated based on a change in the surface emissivity of the heater. The first change was the increasing heater power requirements to reach a desired temperature. The heater power required for the 0.5 hour pre-heat before ignition was measured to be 108.0 W for the first ignition and 117.0 W for the post-test ignition prior to removal of the cathode from the test facility. This change in power requirements may be evaluated according to the following:

$$P_{in} = P_{out} \qquad (1)$$

where P_{in} is the input power to the cathode from the heater and P_{out} is the power lost by the cathode and heater assembly. These power factors can be expressed as:

$$P_{in} = I_{htr} \cdot V_{htr} \qquad (2)$$

$$P_{out} = P_{cond} + P_{rad} \qquad (3)$$

where I_{htr} is the heater current, V_{htr} is the heater voltage, P_{cond} is the power losses via heat conduction, , and P_{rad} is the power lost to radiation.

Since the input power needed to reach the prescribed temperature changed over the wear-test:

$$P_{inf} > P_{ini} \qquad (4)$$

The output power must still be equal to the input power and therefore must also change:

$$\Delta P_{in} = \Delta P_{out} \qquad (5)$$

$$\Delta P_{out} = \Delta P_{cond} + \Delta P_{rad} \qquad (6)$$

If it is assumed that there were no changes in conduction losses over the course of the wear-test, then a change in the radiated power must be responsible for the change in required heater power.

$$\Delta P_{htr} = \Delta P_{rad} = P_{radf} - P_{radi} \qquad (7)$$

where P_{radi} is the radiated power losses at the beginning of the test and P_{radf} is the radiated power losses at the test end. Using the relation for radiated power:

$$P_{rad} = \varepsilon \sigma A T^4 \qquad (8)$$

where ε is the total surface emissivity, σ is the Stefan-Boltzman constant, T is the surface temperature, and A is the area of the radiating surface. Assuming no change in radiating area, then equation 7 becomes:

$$\Delta P_{htr} = \varepsilon_f \sigma A T_f^4 - \varepsilon_i \sigma A T_i^4 \qquad (9)$$

Solving this equation for ε_f:

$$\varepsilon_f = \varepsilon_i (\frac{T_i}{T_f})^4 + \frac{\Delta P_{htr}}{\sigma A T_f^4} \qquad (10)$$

Using the measured data: $T_i = 1050\ ^oC$, $T_f = 1047\ ^oC$, $\Delta P_{htr} = 9.0$ W, the assumed radiating area of the Ta foil surface on the heater of $1.06 \times 10\text{-}3\ m^2$, and an estimated initial surface emissivity of 0.17 for clean tantalum,[18] the post-test emissivity was found to be approximately 0.22.

In order to verify this change in emissivity, the temperature values at the beginning and end of the test were examined. The total input power to the cathode was found to be approximately the same during the test. Assuming that the input power terms (cathode, plasma, and anode) did not change during the test, the power losses from the cathode must have also remained the same. Consequently, if the radiation losses were taken to be constant:

$$P_{radi} = P_{radf} \qquad (11)$$

or, using equation 8 for radiated power, then:

10

$$\varepsilon_i \sigma A T_i^4 = \varepsilon_f \sigma A T_f^4 \qquad (12)$$

Then, solving this equation for the final emissivity:

$$\varepsilon_f = \varepsilon_i (\frac{T_i}{T_f})^4 \qquad (13)$$

With the measured temperatures of 1090 and 1025 ^oC for initial and final values respectively and an assumed initial surface emissivity of 0.17, the resulting final emissivity is approximately 0.21.

The difference between the two final emissivities values was within the uncertainties of the experimental measurements (1% for the thermocouples and power supplies).

Agreement between the two derivations suggested that the change in surface emissivity of the cathode heater may be responsible for the observed changes in cathode tube temperature and heater performance, and therefore was not a result of a change in cathode condition. The negligible change in discharge voltage over the test also suggested a cause unrelated to cathode internal phenomena was responsible for the change in tube temperature. A probable cause of an increase in surface emissivity may have been coating of the Ta foil surfaces during discharge operation from materials in the discharge chamber. Possible sources for a coating were the Sm-Co magnets, fiberglass sheathing used as insulation, and material coming out of the hollow cathode. While no single source was apparent, trace amounts of Si, Ba, Ca, Co, Mo, and Fe were found on a heater insulator surface. In addition, discoloration was observed on all of the internal discharge chamber surfaces which were at anode potential. Further investigation was necessary to verify the emissivity change of the foil and determine the source of coatings.

ACKNOWLEDGEMENTS

REFERENCES

1. Brophy, J.R., and Garner, C.E., "Tests of High Current Hollow Cathodes for Ion Engines," AIAA Paper No. 88-2913, July 1988.

2. Rawlin, V.K., "Internal Erosion Rates of a 10 kW Xenon Ion Thruster," AIAA Paper No. 88-2913, July 1988.

3. Patterson, M.J., and Verhey, T.R., "5 kW Xenon Ion Thruster Lifetest," AIAA Paper No. 90-2543, June 1990.

4. Verhey, T.R., and Patterson, M.J., "Microanalyses of Extended-test Xenon Hollow Cathodes," AIAA Paper No. 91-2123, June 1991.

5. Fearn, D.G., Singfield, A., Wallace, N.C., Gair, S.A., and Harris, P.T., "The Operation of Ion Thruster Hollow Cathodes using Rare Gas Propellants," AIAA Paper No. 90-2584, July 1990.

6. Kitamura, S., Miyazaki, K., and Hiyakawa, Y., "Thousand Hour Test of 14 cm Diameter Ring-Cusp Xenon Ion Thruster," AIAA Paper No. 90-2542, July, 1990.

7. Beattie, J.R., Matossian, J.N., and Robson, R.R., "Status of Xenon Ion Propulsion Technology," AIAA Paper No. 87-1003, May 1987.

8. Brophy, J.R., and Garner, C.E., "A 5,000 hour Xenon Hollow Cathode Life Test," AIAA Paper No. 91-2122, June 1991.

9. DePauw, J.F., "30 cm Thruster Cathode Activation," NASA TRIM No. 13, Dec. 1977.

10. Patterson, M.J., "Performance Characteristics of Ring-Cusp Thrusters with Xenon Propellant," AIAA Paper No. 86-1392, June 1986.

11. Kohl, W.H., Handbook of Materials and Techniques for Vacuum Devices, New York: Reinhold, 1967, pp. 494.

11

12. Fearn, D.G., Cox, A.S., and Moffitt, D.R., "An Investigation of the Initiation of Hollow Cathode Discharges," R.A.E. Technical Report No. 76054, April 1976.

13. Lipeles, R.A., and Kan, H.K.A., "Chemical stability of barium calcium aluminate dispenser cathode impregnants," Appl. Surface Sci., **16**, 1983, pp. 189-206.

14. Kan, H.K.A., Seaver, R.R., Eng, G., and Wachi, F.M., "Generic TWT Development Program Test Cathode A19-10 Analysis," Aerospace Report No. TOR-0089(4404-20)-2, The Aerospace Corp., El Segundo, CA, July 15, 1989.

15. Siegfried, D.E., and Wilbur, P.J., "Studies of an Experimental Quartz Tube Hollow Cathode," IEPC Paper No. 79-2056, July 1979.

16. Stillwell, R.P., Robinson, R.S., Kaufman, H.R., and Cupp, R.K., "Experimental Investigation of an Argon Hollow Cathode," J. Spacecraft & Rocketry, 22, Jan.-Feb., 1985.

17. Suitch, P.R., "Thermochemical reactions in tungsten-matrix dispenser cathodes impregnated with various barium-calcium-aluminates," Doctoral Thesis, Georgia Institute of Technology, Dec. 1987.

18. Kohl, W.H., Handbook of Materials and Techniques for Vacuum Devices, New York: Reinhold, 1967, pp. 303.

Table I. Design specifications of WT-III hollow cathode.

| Element | Parameter Specifications | | |
	Material	Dimensions	Details
Body Tube	Molybdenum-47.5-Rhenium	10.2 cm long x 0.64 cm O.D., with 0.046 cm wall thickness.	
Orifice Plate	Tungsten -2%Thoria	0.62 cm O.D. x 0.13 cm thick.	0.15 cm diameter orifice with 45° half-angle chamfer; e-beam welded to body tube.
Insert	Sintered Tungsten; 80% porosity	2.54 cm long x 0.53 cm O.D., with 0.085 cm wall thickness.	Impregnate: type S, $4BaO\cdot CaO\cdot Al_2O_3$
Insert Collar	Molybdenum	0.2 cm long x 0.53 cm O.D., with 0.085 cm wall thickness.	Attached to insert body with Mo/Ru braze; Re electrical leads brazed to collar.
Heater	Tantalum sheath, magnesium oxide insulator, tantalum inner conductor. Tantalum foil radiation shielding.	46 cm length uncoiled; helical coil of 8 turns formed. 12 layers of 0.013 mm thick foil wrapped over coiled section.	One end of inner conductor connected to outer Ta sheath.

Table II. Comparison of test-system configurations, procedures and operating parameters of the three wear-test cathodes.

| Property | Cathode Wear-tests | | |
	WT-I	WT-II	WT-III
Feed-system Tubing Length/type	10.2 m of standard 304 stainless steel 0.64 cm dia. + 1 m of 0.33 cm teflon tubing.	3.4 m of 0.64 cm dia. and 4.0 m of 0.77 cm dia. standard 304 stainless steel tubing.	2.54 m of 0.64 cm dia. electro-polished 316L stainless steel tubing.
Fitting type	Pressure compression seal	High vacuum metal compression gasket	Ultra high vacuum metal gasket seals and welded
Vacuum pump	Oil Diffusion	Oil Diffusion	He Refrigerator Cryo-pump
Feed-system bake-out	None	None	17 hours @ 75 $^{\circ}$C
Gas Purifier	None	None	O_2 & H_2O getter
Feed-system Leak-rate, Pa-L/s	6.2×10^{-4}	1.1×10^{-4}	4.0×10^{-6}
Test configuration	Cylindrical anode with keeper-like ignitor .	Cylindrical anode.	Discharge chamber simulator with magnetic field.
Activation procedure	Procedure outlined in Ref. 3.	SEPS-based (Ref. 4)	SEPS-based (Ref. 4)
Test Parameters; average value ± standard deviation over test duration.			
Emission Current, A	23.0	23.0	23.0
Discharge Voltage, V	17.9 ± 2.1	19.7 ± 1.6	16.7 ± 0.15
Cathode Tube Temperature, $^{\circ}$C from thermocouple. ±1%	1160 ± 39	1100 ±13	1050 ± 18
Xenon Mass Flow Rate, Pa-L/s (sccm) ± 2.5%	10.0 (6.1)	10.0 (6.1)	10.0 (6.1)
Ignition Voltage, V/Xenon mass flow rate ,Pa-L/s	<400/46.0	25-100/17.0	21/17.0
Test Duration, hours	504	478	508
No. of Test Shutdowns	1	2	2

Table III. Comparison of the observed changes and phenomena of three wear-test cathodes.

Change/ Phenomenon	Cathode Wear-tests		
	WT-I	**WT-II**	**WT-III**
Orifice chamfer and channel	Some tungsten metal deposition on surfaces; no obstruction.	Free of tungsten deposition.	Free of tungsten deposition.
Interior surface of orifice plate	Large tungsten deposition around orifice plate; extended from orifice to insert deposition edge.	Small ring of tungsten deposited around orifice.	Very small (100 μm wide) ring of tungsten metal deposited around orifice; tungsten particles with Ba & Ca deposited on rest of surface.
Insert surface:			
Downstream surface	Large tungsten metal deposition formed; surface roughened next to deposition.	Small whisker formation on downstream edge; $BaWO_4$ found.	Small increase in surface porosity of sintered tungsten.
Middle	Large amorphous BA-Ca-W-Al-O insulating layer formed over large area; $BaWO_4$ found.	Azimuthal ring (~0.1 cm wide) of amorphous Ba-W-Ca-Al-M0-O insulating coating.	No change in surface condition.
Upstream surface	Tungsten detected, but not in sintered form.	Ba-Ca-W-Al-Mo-O coating formed over surface.	Ba-Ca-Al coating and Ca crystal formations found, Ba_2CaWO_6 found.
Cathode Tube-Insert Gap	Impregnate-based compound formed which affixed insert into cathode.	Impregnate-based material found on inner cathode tube wall; insert was removable.	Impregnate-based compound formed in gap; insert was removable.
Insert Collar	Not examined	Whisker formation found at collar-cathode tube junction.	Impregnate-based material deposited on surface.
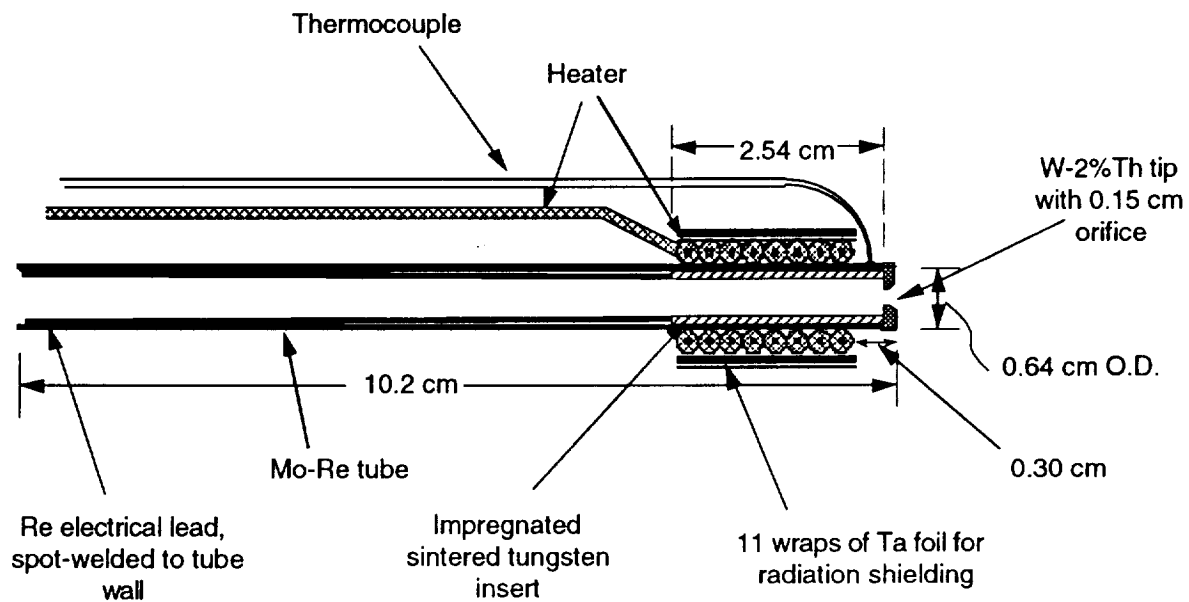
Figure 1. Schematic of WT-III Hollow Cathode.
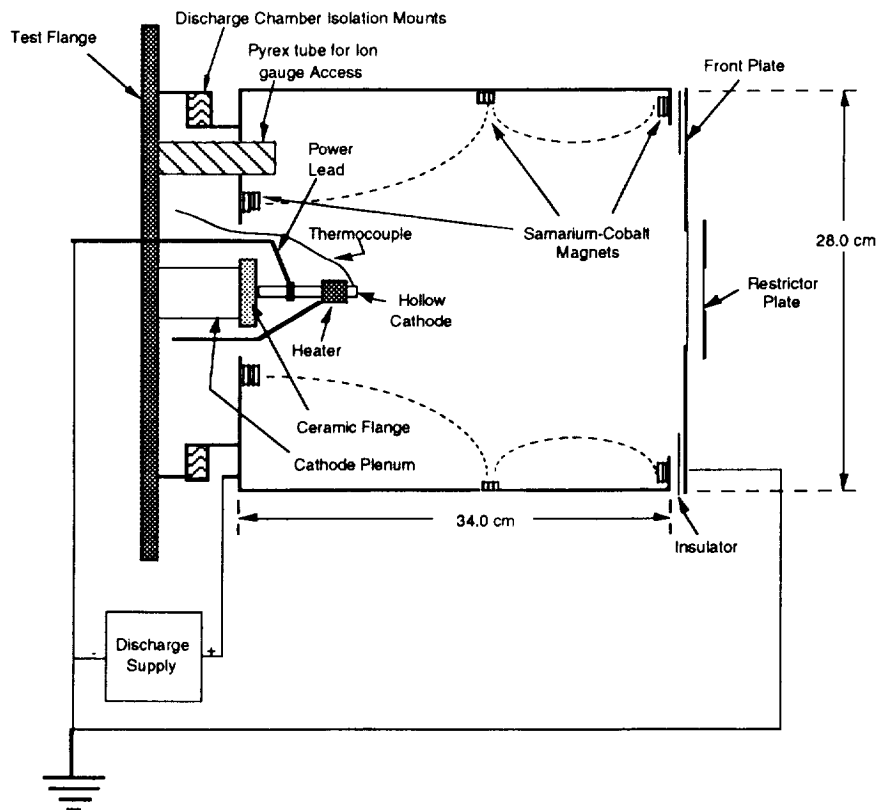
Figure 2. Schematic of Discharge Chamber Simulator. Electrical schematic for discharge supply is also shown.
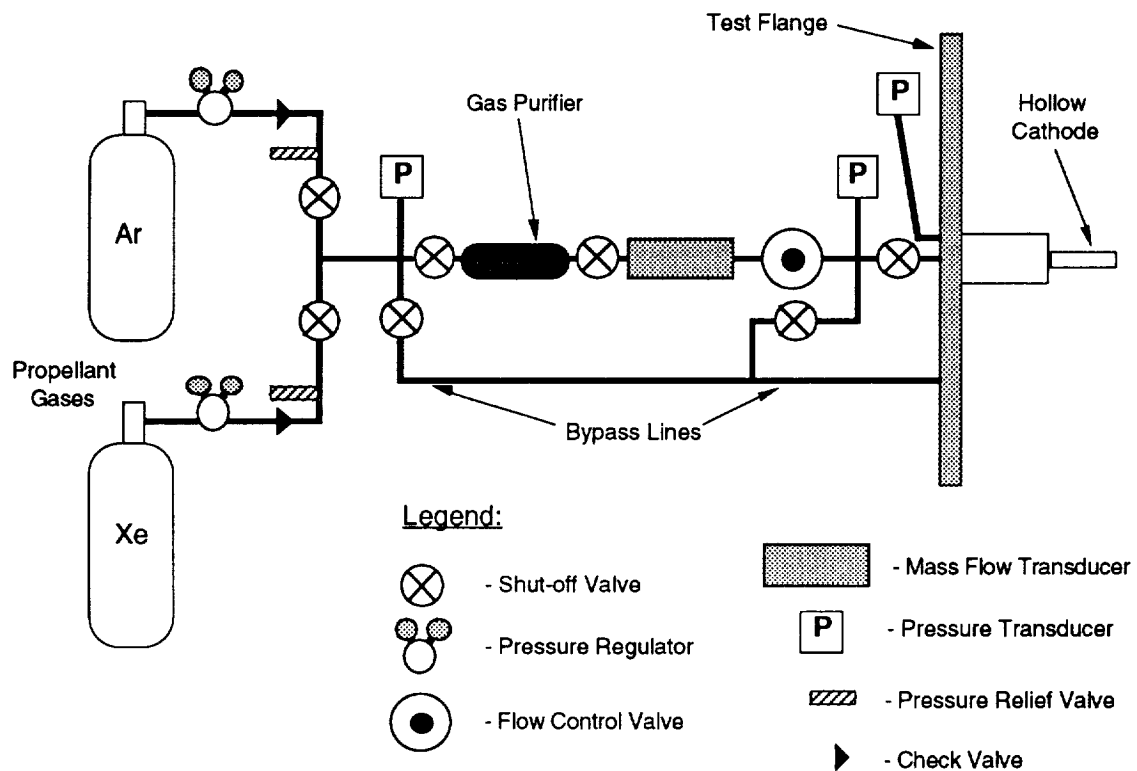
15

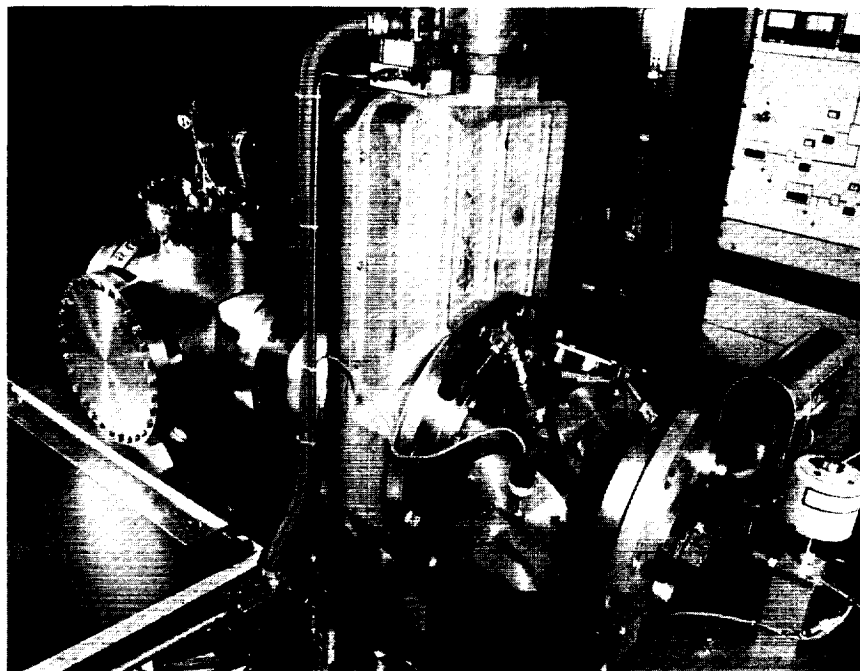Figure 3. Schematic of Propellant Feed-system.

Figure 4. Photograph of Hollow Cathode Wear-testing Facility.
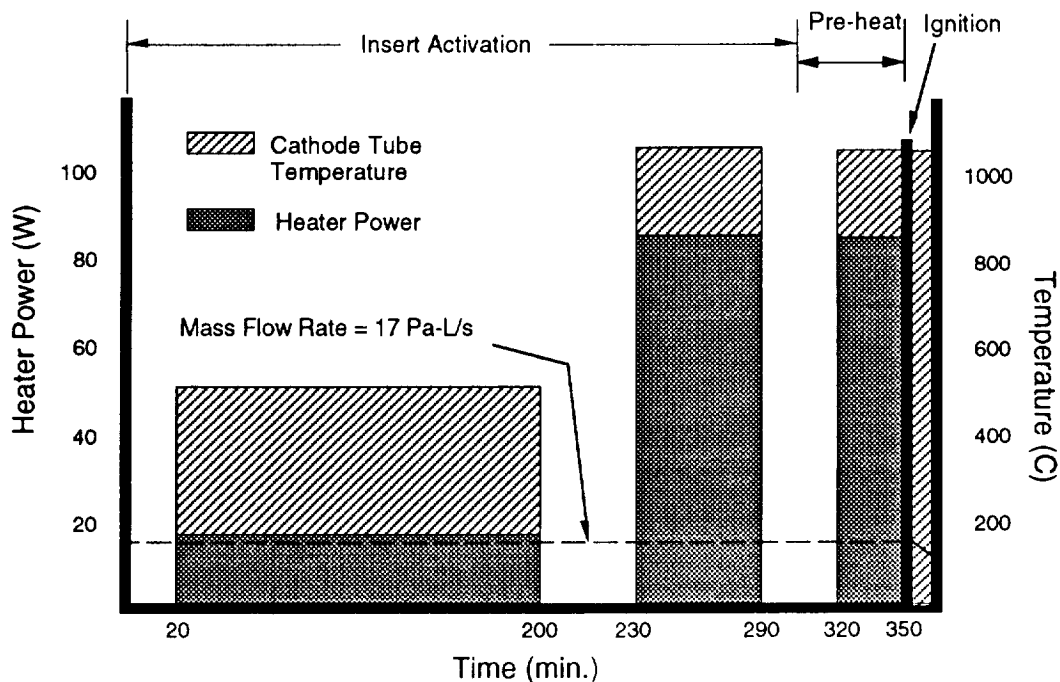
Figure 5. Schematic of the Heater Power and Cathode Temperature Requirements for the Hollow Cathode Activation, Pre-heat, and Ignition Procedures.
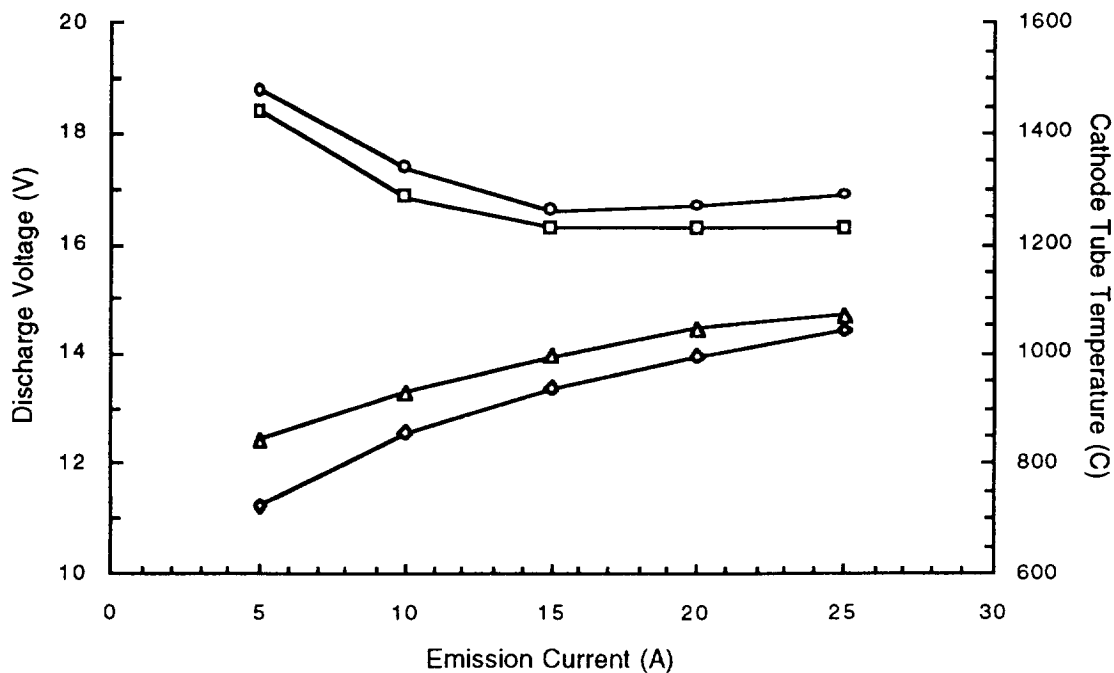

Figure 6. Plot of Discharge Voltage and Cathode Temperature versus Emission Current before and after wear-test WT-III. □ - pre-test discharge voltage, O - post-test discharge voltage, △ - pre-test cathode tube temperature, ◇ - post-test cathode tube temperature.

17
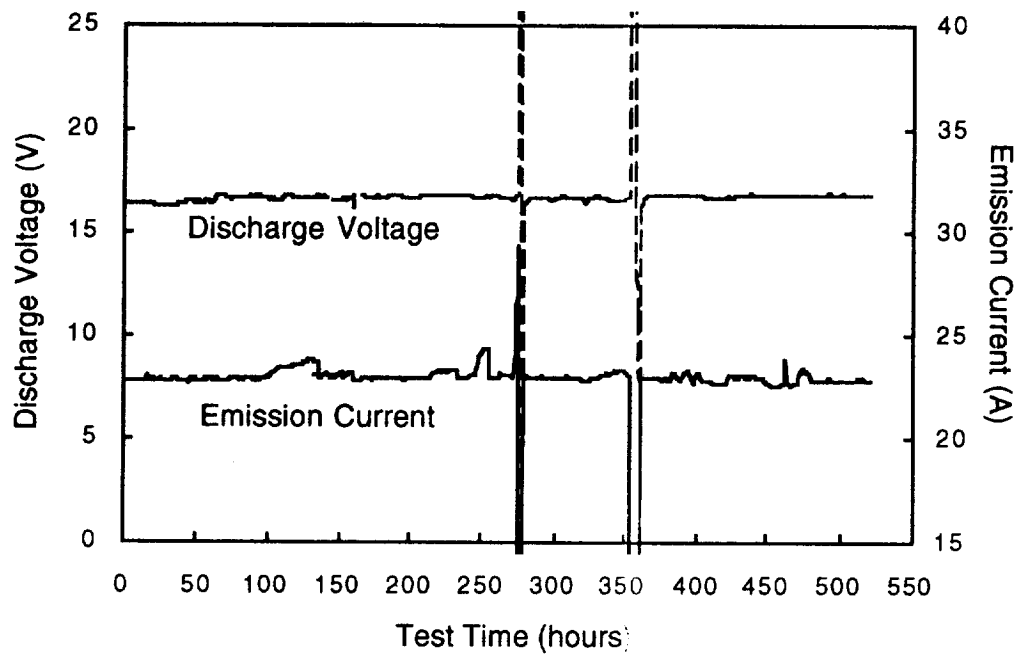
Figure 7. Hollow Cathode Discharge Voltage and Emission Current during wear-test WT-III. The two spiked regions indicate the occurrence of test shutdowns.
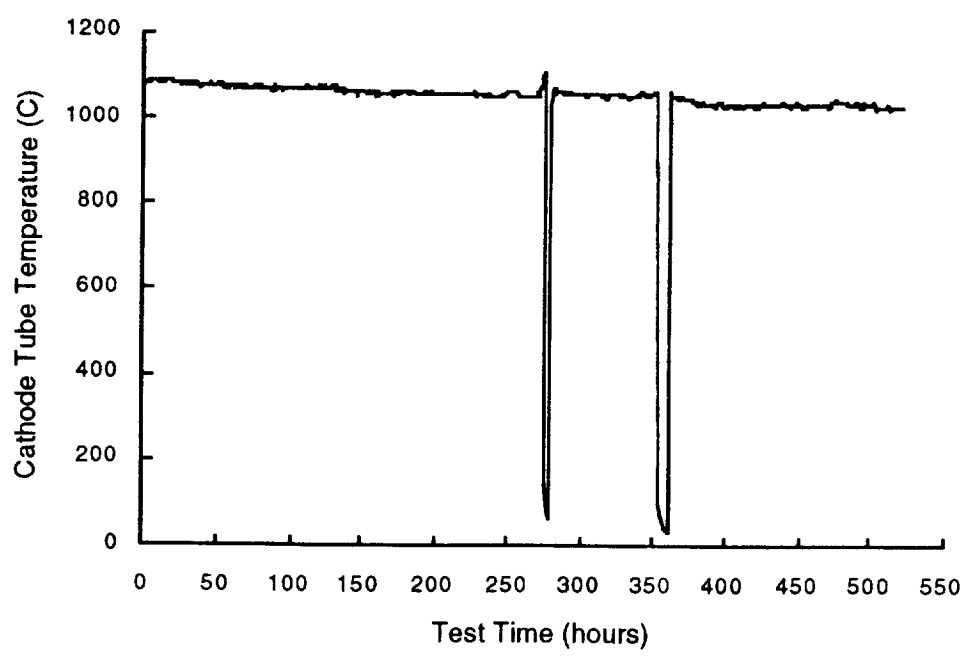
Figure 8. Cathode tube temperature during wear-test WT-III as measured with a thermocouple. The two spiked regions indicated the occurrence of test shutdowns.
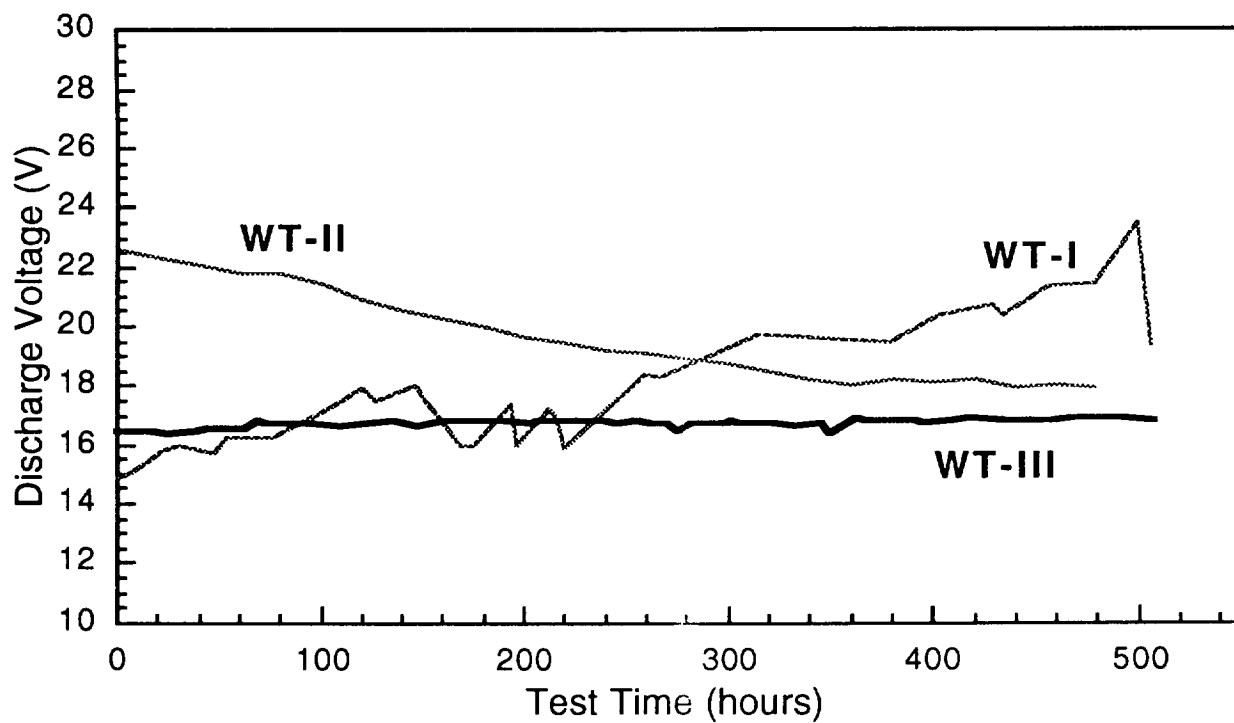
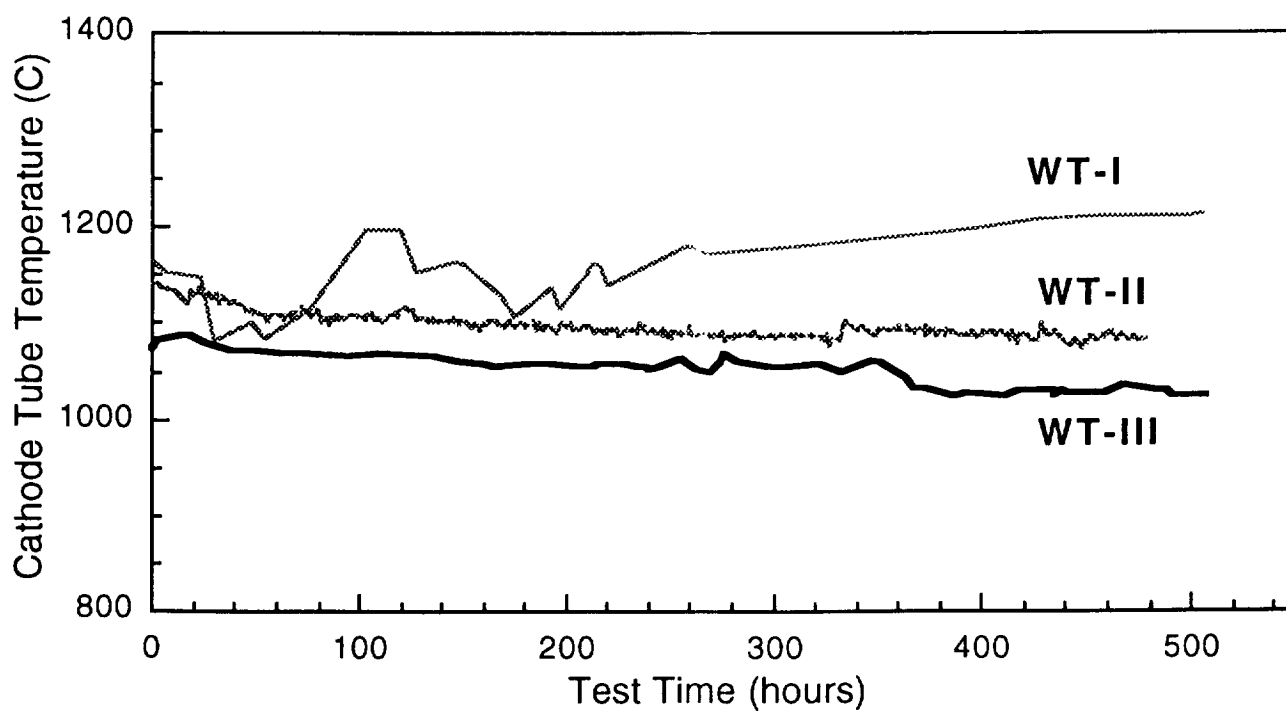Figure 9. Discharge voltage versus time for three wear-tests; WT-I, WT-II and WT-III.

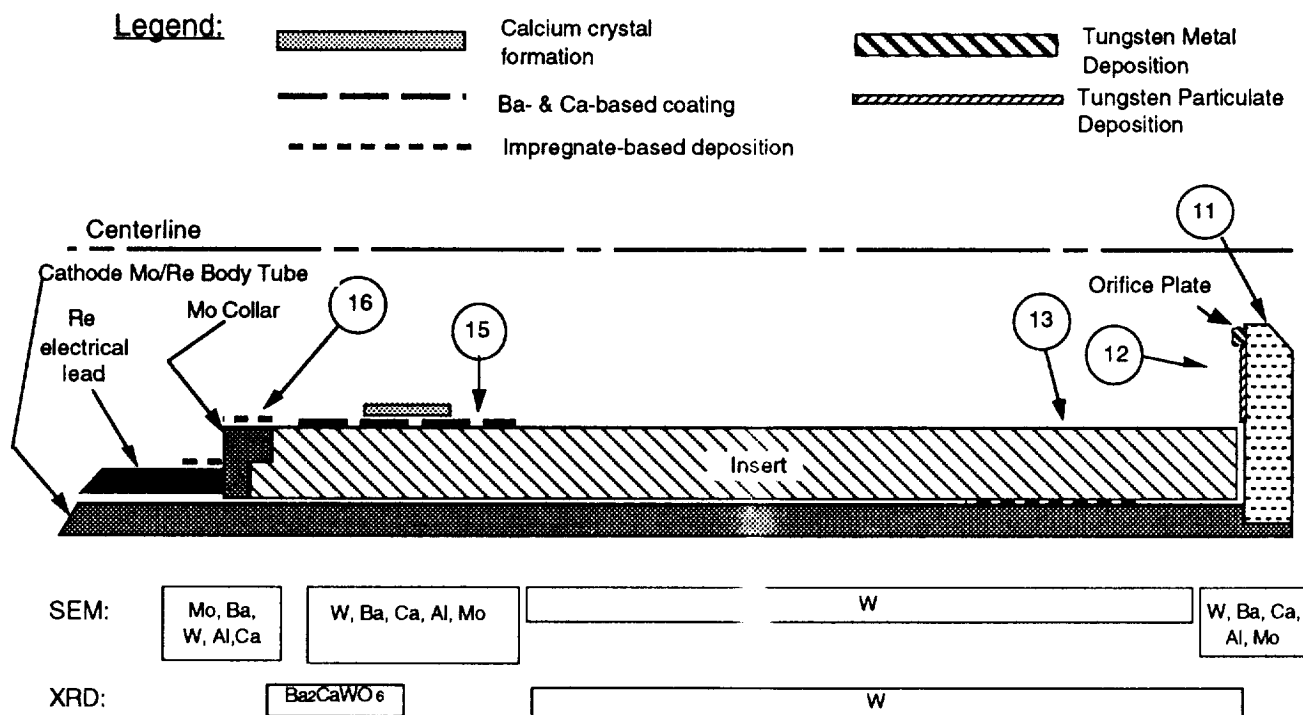Figure 10. Cathode temperature versus time for three wear-tests; WT-I, WT-II, and WT-III.

Legend:

▨ Calcium crystal formation

— — — Ba- & Ca-based coating

▬ ▬ ▬ ▬ Impregnate-based deposition

▨ Tungsten Metal Deposition

▨ Tungsten Particulate Deposition

Centerline

Cathode Mo/Re Body Tube

Re electrical lead

Mo Collar

Orifice Plate

Insert

11

16

15

13

12

SEM:	Mo, Ba, W, Al,Ca	W, Ba, Ca, Al, Mo	W	W, Ba, Ca, Al, Mo

XRD:	Ba_2CaWO_6	W

Figure. 11. Schematic diagram of cathode insert cross-section indicating qualitative changes in cathode condition. Schematic is not to scale. Encircled figure numbers indicate location of SEM photographs.

a) Pre-test.
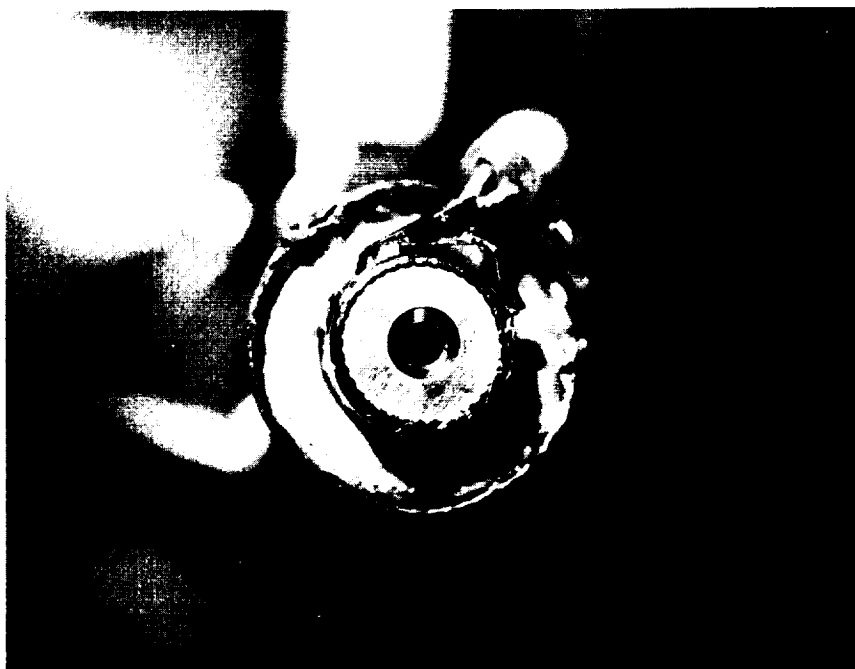
b). Post-test.
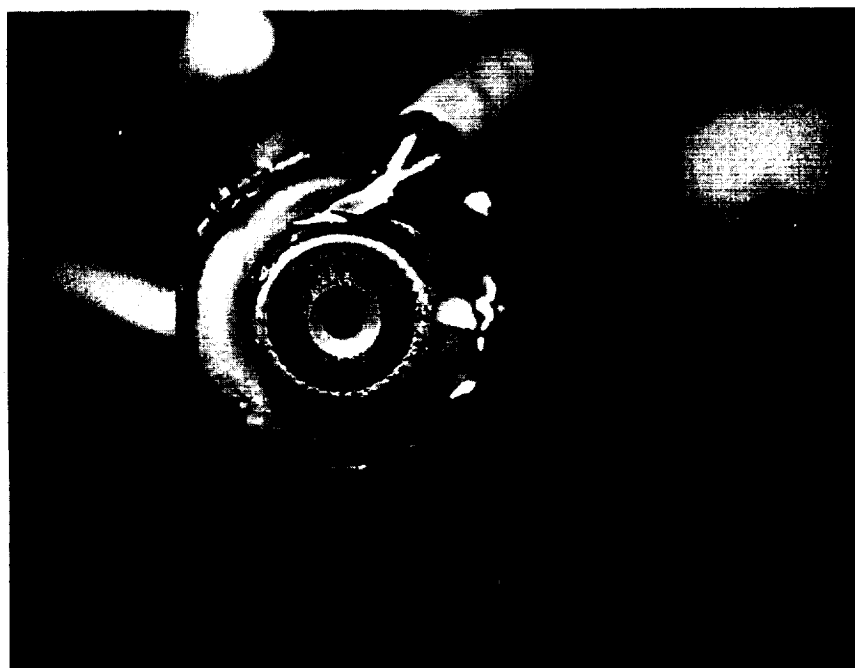
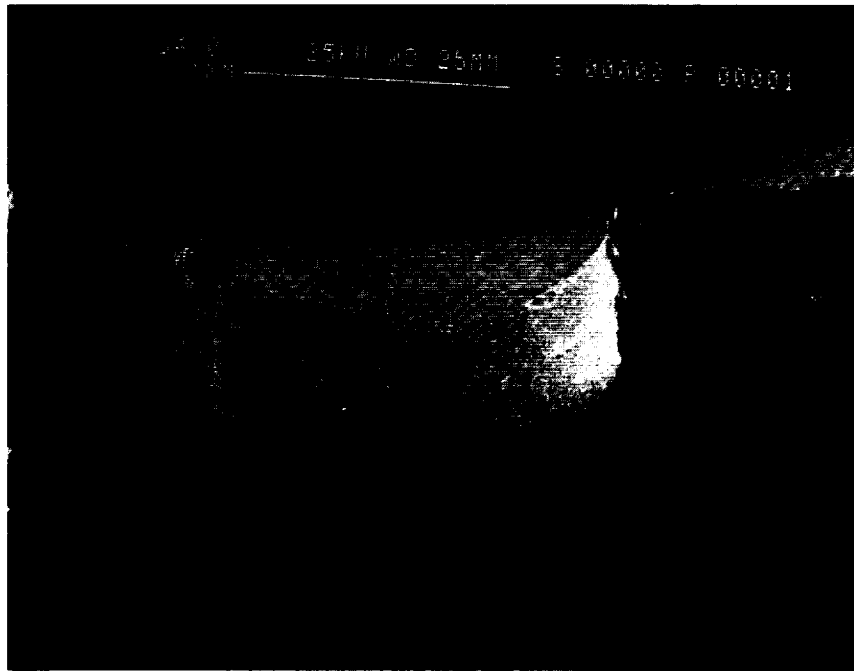Figure 12. Photograph of the cathode WT-III orifice plate.

Figure 13. WT-III hollow cathode orifice. Direction of gas flow was top to bottom.

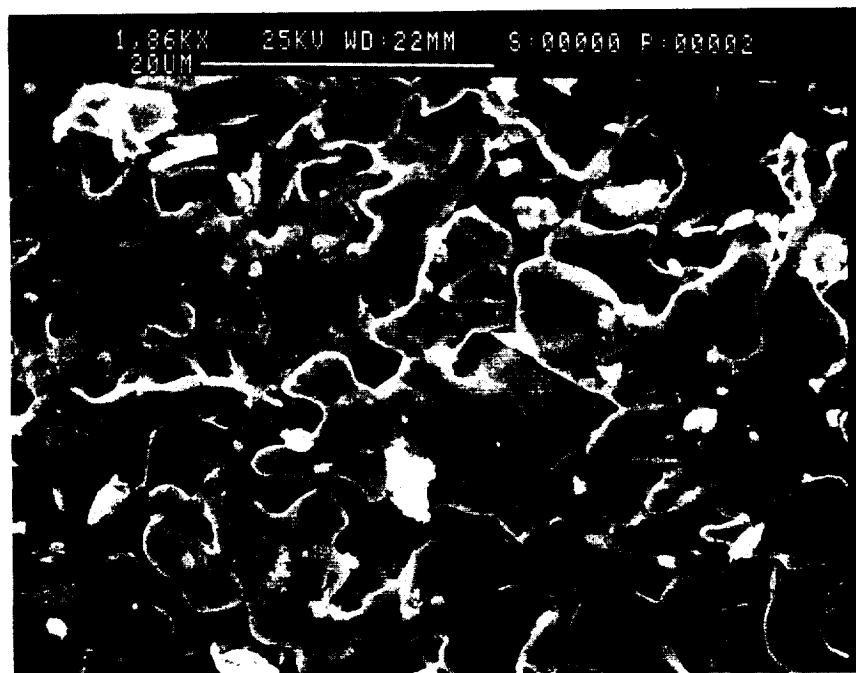Figure 14. Photograph of WT-III orifice plate interior surface.

22

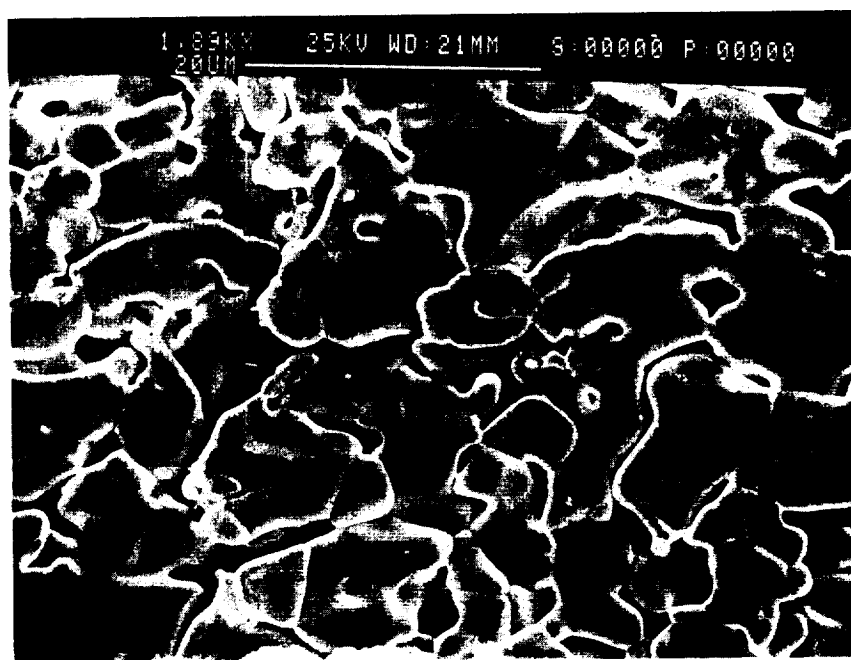Figure 15. Downstream region of WT-III insert surface.

Figure 16. Surface of an untested, unactivated insert.

23

Figure 17. Backscattered electron image of upstream region of WT-III insert surface.
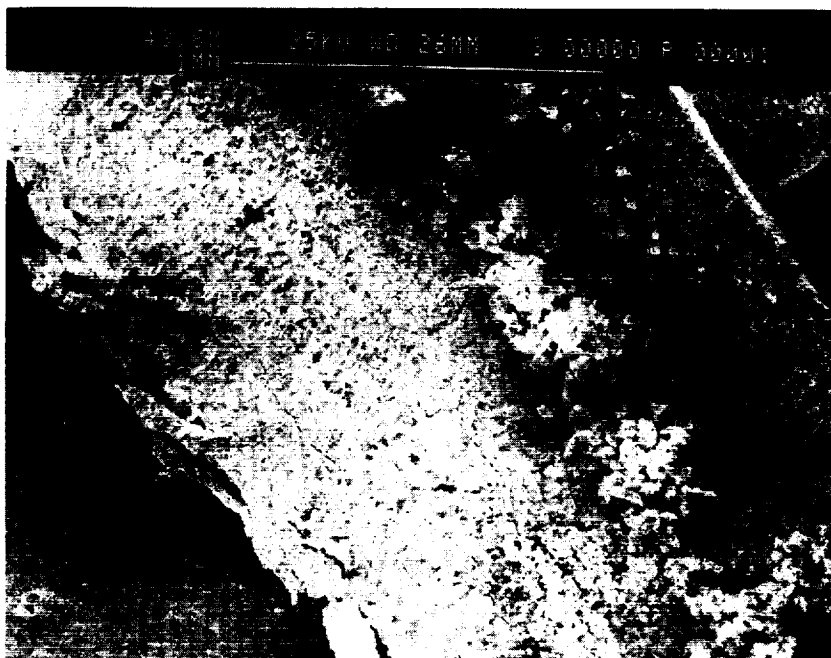

Figure 18. Deposited structure on the Mo collar upstream of WT-III insert surface.

24

REPORT DOCUMENTATION PAGE

Public reporting burden for this collection of information is estimated to average 1 hour per response, including the time for reviewing instructions, searching existing data sources, gathering and maintaining the data needed, and completing and reviewing the collection of information. Send comments regarding this burden estimate or any other aspect of this collection of information, including suggestions for reducing this burden, to Washington Headquarters Services, Directorate for information Operations and Reports, 1215 Jefferson Davis Highway, Suite 1204, Arlington, VA 22202-4302, and to the Office of Management and Budget, Paperwork Reduction Project (0704-0188), Washington, DC 20503.

1. AGENCY USE ONLY (Leave blank)	2. REPORT DATE	3. REPORT TYPE AND DATES COVERED
	July 1992	Final Contractor Report

4. TITLE AND SUBTITLE

Extended-Testing of Xenon Ion Thruster Hollow Cathodes

5. FUNDING NUMBERS

WU–506–42–31

6. AUTHOR(S)

Timothy R. Sarver-Verhey

7. PERFORMING ORGANIZATION NAME(S) AND ADDRESS(ES)

Sverdrup Technology, Inc.
Lewis Research Center Group
2001 Aerospace Parkway
Brook Park, Ohio 44142

8. PERFORMING ORGANIZATION REPORT NUMBER

E–7279

9. SPONSORING/MONITORING AGENCY NAMES(S) AND ADDRESS(ES)

National Aeronautics and Space Administration
Lewis Research Center
Cleveland, Ohio 44135–3191

10. SPONSORING/MONITORING AGENCY REPORT NUMBER

NASA CR–189227
AIAA–92–3204

11. SUPPLEMENTARY NOTES

Prepared for the 28th Joint Propulsion Conference and Exhibit cosponsored by the AIAA, SAE, ASME, and ASEE, Nashville, Tennessee, July 6–8, 1992. Timothy R. Sarver-Verhey, Sverdrup Technology, Inc., Lewis Research Center Group, Brook Park, Ohio 44142. Project Manager, James S. Sovey, Low Thrust Propulsion Branch, NASA Lewis Research Center, (216) 433–7454.

12a. DISTRIBUTION/AVAILABILITY STATEMENT

Unclassified - Unlimited
Subject Category 20

12b. DISTRIBUTION CODE

13. ABSTRACT (Maximum 200 words)

A hollow cathode wear-test of 508 hours was successfully completed at an emission current of 23.0 A and a xenon flow rate of 10 Pa-L/s. This test was the continuation of a hollow cathode contamination investigation. Discharge voltage was stable at 16.7 V. The cathode temperature averaged 1050 °C with a 7% drop during the wear-test. Discharge ignition voltage was found to be approximately 20 V and was repeatable over four starts. Post-test analyses of the hollow cathode found a much improved internal cathode condition with respect to earlier wear-test cathodes. Negligible tungsten movement occurred and no formation of mono-barium tungsten was observed. These results correlated with an order-of-magnitude reduction in propellant feed-system leakage rate. Ba_2CaWO_6 and extensive calcium crystal formation occurred on the upstream end of the insert. Ba-Ca compound depositions were found on the Mo insert collar, on the Re electrical leads, and in the gap between the insert and cathode wall. This wear-test cathode was found to be in the best internal condition and had the most stable operating performance of any hollow cathode tested during this contamination investigation.

14. SUBJECT TERMS

Electric propulsion; Inert gases; Ion thruster; Plasma/electron source: Hollow cathodes

15. NUMBER OF PAGES

26

16. PRICE CODE

A03

17. SECURITY CLASSIFICATION OF REPORT	18. SECURITY CLASSIFICATION OF THIS PAGE	19. SECURITY CLASSIFICATION OF ABSTRACT	20. LIMITATION OF ABSTRACT
Unclassified	Unclassified	Unclassified	

NSN 7540-01-280-5500

Standard Form 298 (Rev. 2-89)
Prescribed by ANSI Std. Z39-18
298-102